Published in final edited form as:

Neuron. 2016 May 4; 90(3): 507–520. doi:10.1016/j.neuron.2016.03.016.

PIAS1 regulates mutant Huntingtin accumulation and Huntington's disease-associated phenotypes in vivo

Joseph Ochaba[1], **Alex Mas Monteys**[2], **Jacqueline G. O'Rourke**[3], **Jack C. Reidling**[4], **Joan S. Steffan**[4,6], **Beverly L. Davidson**[2,6], and **Leslie M. Thompson**[1,4,6,*]

[1]Department of Neurobiology and Behavior, University of California, Irvine, Irvine, CA 92697, USA

[2]Raymond G. Perelman Center for Cellular and Molecular Therapeutics, The Children's Hospital of Philadelphia, Philadelphia, PA 19104, USA

[3]Cedars-Sinai Medical Center, Board of Governors Regenerative Medicine Institute, Los Angeles, CA 90048, USA

[4]Institute of Memory Impairments and Neurological Disorders, University of California, Irvine, Irvine, CA 92697, USA

[5]Department of Psychiatry and Human Behavior, University of California, Irvine, Irvine, CA 92697, USA

[6]Department of Pathology and Laboratory Medicine, The University of Pennsylvania, Philadelphia, PA 19104, USA

SUMMARY

The disruption of protein quality control networks is central to pathology in Huntington's disease (HD) and other neurodegenerative disorders. The aberrant accumulation of insoluble high molecular weight protein complexes containing the Huntingtin (HTT) protein and SUMOylated protein corresponds to disease manifestation. We previously identified a HTT selective E3 SUMO ligase, PIAS1, which regulates HTT accumulation and SUMO modification in cells. Here we investigated whether PIAS1 modulation in neurons alters HD-associated phenotypes *in vivo*. Instrastriatal injection of a PIAS1-directed miRNA significantly improved behavioral phenotypes in rapidly progressing mutant HTT (mHTT) fragment R6/2 mice. PIAS1 reduction prevented the accumulation of mHTT, SUMO- and ubiquitin-modified proteins, increased synaptophysin levels, and normalized key inflammatory markers. In contrast, PIAS1 overexpression exacerbated mHTT-associated phenotypes and aberrant protein accumulation. These results confirm the association

*Contact: lmthomps@uci.edu.

Designed the experiments: J.O., A.M.M., J.G.O., J.C.R., J.S.S., B.L.D., L.M.T.
Carried out experiments: J.O., A.M.M., J.G.O.
Analyzed the data: J.O., A.M.M., J.C.R., J.S.S., B.L.D., L.M.T.
Wrote the manuscript: J.O., A.M.M., J.S.S., B.L.D., L.M.T.

between aberrant accumulation of expanded polyglutamine-dependent insoluble protein species to pathogenesis and link phenotypic benefit to reduction of these species through PIAS1 modulation.

INTRODUCTION

Huntington's disease (HD) is caused by an expansion of a CAG repeat within the HD gene, encoding an expanded stretch of polyglutamines in the Huntingtin (HTT) protein (The Huntington's Disease Collaborative Research Group, 1993). Symptoms include movement abnormalities, psychiatric symptoms and cognitive deficits with accompanying cortical atrophy and degeneration of medium spiny neurons in the striatum (Ross and Tabrizi, 2011). A key pathological feature is the aberrant accumulation of mutant HTT (mHTT) protein (Waelter et al., 2001), potentially through the disruption of protein quality control networks that ensure proper folding and degradation of cellular proteins (La Spada and Taylor, 2010; Wilkinson et al., 2010). Post-translational modifications (PTMs) of HTT, including SUMOylation and phosphorylation (Ehrnhoefer et al., 2011; Pennuto et al., 2009), may contribute to mechanisms underlying mHTT accumulation (O'Rourke et al., 2013; Thompson et al., 2009) and influence *in vivo* pathogenesis (Gu et al., 2005). Additionally, SUMO modification itself can function as a secondary signal affecting ubiquitin-dependent degradation by the proteasome (UPS) (Praefcke et al., 2012).

SUMOylation is the covalent attachment of a Small Ubiquitin MOdifier Protein (SUMO) to target proteins. Although a transient modification, SUMOylation has long-lasting effects, including the regulation of subcellular localization, protein stability and clearance, chromatin remodeling, and interaction properties of modified proteins (Cubenas-Potts and Matunis, 2013; Gareau and Lima, 2010). Four different forms, SUMO 1–4, exist. The SUMOylation pathway involves a cascade of enzymes, with an E1-activating enzyme (SAE1/UBA2), an E2-conjugating enzyme (UBC9), and multiple E3-ligating enzymes (Protein Inhibitors of Activated STAT [PIAS], PC2, MMS21, and RanBP2) which provide substrate specificity. The diversity of SUMO substrates is governed by a relatively small number of SUMO E3 ligases. SUMO modification can occur on the same lysine residue as ubiquitination with extensive crosstalk in regulating cellular protein clearance. More recently, the importance of the SUMO modification system in brain has emerged, given the number of neurotransmitters and receptors that are regulated by SUMOylation (Sen and Snyder, 2010). Further, SUMO proteins are implicated in a growing number of neurodegenerative diseases including Alzheimer's disease, Parkinson's disease, Amyotrophic lateral sclerosis, polyglutamine repeat diseases, and transient cerebral ischemia, as well as HD (Hickey et al., 2008; Datwyler et al., 2011; Krumova and Weishaupt, 2013), typically through an association with dysregulated disease protein aggregation and abundance.

We previously showed that SUMO-1/-2 modified proteins accumulate in an insoluble protein fraction from human HD postmortem striatum, and that SUMO isoforms can regulate the formation and accumulation of this insoluble HTT species in cells (O'Rourke et al., 2013). Both wild type and mHTT are SUMO-1 and 2 modified within the amino terminal 17 amino acids and at downstream sites within the full-length protein (O'Rourke et

al., 2013; Steffan et al., 2004). Modulation of the SUMO network *in vivo* to investigate functional consequences in HD related systems can either be through SUMO itself, which would be anticipated to have an overly broad impact and potentially deleterious effects, or through more selective means such as regulation of a relevant SUMO E3 ligase.

Five major PIAS isoforms are expressed in mammals and can act as adaptor proteins that bridge the SUMO-conjugated E2 enzyme and the substrate in the SUMOylation cascade as well as act as ligases. The PIAS proteins themselves were originally characterized by their ability to regulate transcription, immune responses, and cytokine signaling (Liu and Shuai, 2008; Rytinki et al., 2009), although roles in protein clearance pathways are emerging (Lee et al., 2009; Liu and Shuai, 2009). We previously demonstrated that PIAS1 can selectively enhance HTT modification by both SUMO-1 and SUMO-2 and regulate the formation of insoluble high molecular weight (HMW) HTT species, suggesting that PIAS1 might influence pathogenesis in HD. Further, genetic reduction of the single dPIAS in mHTT-expressing *Drosophila* is protective (O'Rourke et al., 2013).

Given the ability of PIAS1 to enhance SUMO modification of HTT and regulate mHTT accumulation in cell models, we hypothesized that reduction of PIAS1 in HD striata might confer neuroprotection. Using viral delivery of a mouse PIAS1-targeting artificial microRNA (miRNA) to the HD modeled R6/2 mouse striatum, which shows progressive accumulation of HMW mHTT protein, PIAS1 reduction significantly prevented HD-associated phenotypes and accumulation of insoluble mHTT. Strikingly, PIAS1 ameliorated disease-associated increases in apparent microglial activation and dysregulation of relevant proinflammatory cytokines. Conversely PIAS1 overexpression exacerbated disease phenotypes and the accumulation/aggregation profile. These results suggest that PIAS1 may link protein homeostasis, neuroinflammation and disease symptomatology by modulating formation of toxic forms of accumulated mHTT.

RESULTS

Targeted modulation of PIAS1 in the striatum of mHTT expressing R6/2 mice

To investigate the relationship between mHTT accumulation and functional outcomes and determine whether PIAS1 contributes to this network *in vivo*, we used acute instrastriatal knockdown or overexpression of PIAS1 in a mHTT expressing mouse model. PIAS1 protein is expressed in most tissues including brain therefore we confined knockdown to the brain. Our studies utilized R6/2 transgenic mice, based on their relatively rapid progression, the formation of detergent-insoluble aggregated species of HTT which increase with disease progression, and inflammatory responses that are reminiscent of symptomatic human HD (Chang et al., 2015; Hsiao et al., 2013). These mice express the first exon of human HTT (CAG repeat of ~125), and show reproducible and rapidly progressing motor and metabolic symptoms at 6 weeks of age and eventually develop tremors, lack of coordination, excessive weight loss, and early death (~12 weeks) (Mangiarini et al., 1996).

Adeno-associated viruses, which transduce striatal neurons (AAV2/1 or 2/2) (Harper et al., 2005; McBride et al., 2008), were engineered to express PIAS1-targeting artificial miRNAs for acute knockdown of PIAS1 *in vivo*. A series of mouse PIAS1-directed artificial miRNAs

were tested and miPIAS1.3 selected based on optimal knockdown in NIH3T3 cells (Figure S1A–B. Related to Figure 1). Striata of mice were bilaterally injected with rAAV2/1miPIAS1.3-CMVeGFP (miPIAS1.3) or rAAV2/1-mU6miSAFE-CMVeGFP (miSAFE) (mismatch control) for knockdown studies and rAAV2/2-CMVPIAS1 (PIAS1) or rAAV2/2-CMVeGFP (eGFP) (viral control) for overexpression studies at 5 weeks of age. For knockdown studies, mice were sacrificed at 10 weeks. PIAS1 overexpression mice were sacrificed at 9 weeks due to declining health of mice. Consistent with other studies (Aschauer et al., 2013; Harper et al., 2005; McBride et al., 2008), AAV2/1 and 2/2 viral transduction was neuronal as demonstrated by βIII-tubulin/eGFP co-localization and lack of GFP expression in microglia or astrocytes as measured by Iba1 or GFAP co-staining (Figures 1A–B).

PIAS1 protein levels were evaluated to determine whether modulation was achieved in treated mice following viral injections. We previously showed that PIAS1 is primarily in the detergent-insoluble fraction, similar to HMW HTT and modified proteins (O'Rourke et al., 2013), therefore isolated detergent-soluble and detergent-insoluble proteins were evaluated. The detergent-soluble fraction contains mainly cytoplasmic proteins such as GAPDH, monomeric forms of HTT (including the R6/2 mHTT fragment encoding human transgene), endogenous mouse full-length HTT, and soluble oligomeric species of HTT which do not fully resolve on standard PAGE gels (O'Rourke et al., 2013; Sontag et al., 2012) (Figure S2. Related to Figure 3). In contrast, the detergent-insoluble fraction contains primarily nuclear proteins including Histone H3 (Figure S2. Related to Figure 3), HMW HTT species (likely multimers or potentially insoluble oligomers and fibrils), and accumulated forms of SUMO- and ubiquitin-modified proteins. Levels of PIAS1, primarily a nuclear protein, were monitored in striatal tissues from 10 week old R6/2 and non-transgenic (NT) mice. In the soluble fraction, PIAS1 levels are slightly higher in NT animals by Western analysis (Figure S3A. Related to Figure 1), however PIAS1 protein levels were significantly elevated in the insoluble, nuclear fraction from R6/2 mice (Figure S3A. Related to Figure 1). In miPIAS1.3 treated R6/2 mice, insoluble PIAS1 levels in the striatum were markedly reduced, as indicated by decreased protein expression at 5 weeks post-injection relative to miSAFE treated R6/2 mice (Figure 1C). While there was a significant decrease in levels of soluble PIAS1 in NT mice with miPIAS1.3 injection, there was little to no impact on soluble PIAS1 levels in R6/2 mice (Figure S3B. Related to Figure 1). Given the already high levels of PIAS1 in R6/2 mice, miPIAS1.3 miRNA produced a relatively greater apparent degree of knockdown compared to NT mice. As a control for off-target viral effects, we found that apart from eGFP expression, vehicle treated (Formulation Buffer 18) mice did not differ biochemically nor behaviorally from miSAFE treated mice (Figure S4A–C. Related to Figure 2). Given the relatively low levels of insoluble PIAS1 in NT mice, miPIAS1.3 miRNA produced a relatively smaller apparent degree of knockdown compared to R6/2 mice, therefore no statistically significant decrease in PIAS1 levels was detected following miPIAS1.3 treatment in NT mice (Figure 1C). However, knockdown was observed in RNA from both R6/2 and NT mouse striata (Figure S5. Related to Figure 1). For overexpression studies, virus expressing PIAS1 bilaterally injected into R6/2 mouse striata resulted in a significant increase in insoluble PIAS1 levels 4 weeks post-injection (Figure 1D), a

significant reduction in soluble PIAS1 levels was found in NT mice, but not R6/2 mice (Figure S3B. Related to Figure 1).

Modulation of PIAS1 alters behavioral phenotypes in the R6/2 mouse model of HD

R6/2 mice show progressive weight loss, abnormal hind limb posture/splayed limbs when held by the tail (clasping) (Mangiarini et al., 1996), loss of motor coordination and balance measured using a Rotarod test (Carter et al., 1999), a decrease in sensorimotor performance when climbing down a vertical pole (Hickey et al., 2008) and diminished forelimb grip strength (Woodman et al., 2007). To determine whether altering PIAS1 levels *in vivo* had an effect on these R6/2 phenotypes, we injected rAAV virus that either knocks down or overexpresses PIAS1 into the striatum of 5 week old mice and then monitored their body weight and ability to perform on a series of behavioral tasks (Figure 2A).

R6/2 mice begin losing weight and show a decline in behavioral tests at 6 weeks (Mangiarini et al., 1996) and our results are consistent with those findings. No treatment effect on weight was observed for either PIAS1 knockdown or overexpression (Figure S6A–B. Related to Figure 2). Reduction of endogenous levels of PIAS1 in R6/2 mice caused a significant improvement on Rotarod performance compared to miSAFE injected mice at 7 weeks (Figure 2B), but deficits reappeared at 9 weeks (Figure S7. Related to Figure 2). In the pole test task there was no effect observed with miPIAS treated R6/2 mice at 6 weeks, however, by 8 weeks of age they exhibited a complete rescue in deficits observed compared to miSAFE treated R6/2 mice that was comparable to NT mice (Figure 2C). When grip strength was measured, R6/2 mice injected with miPIAS1.3 had no treatment effect at 6.5 weeks, but had a significant and almost complete rescue effect by 8 weeks compared to miSAFE treated R6/2 mice (Figure 2D). Finally, miPIAS1.3 delayed the onset of clasping in R6/2 mice relative to miSAFE treated R6/2 mice (Figure 2E), which persisted up to the 9 week end point. CAG repeat length variability did not account for the behavioral improvement as repeat lengths assessed in a subset of animals (tail and striatal tissue) are within a tight range of 122–132 CAGs across animals with variation between individual animal tail samples and striatal tissue within 1–2 CAG repeats.

Next, we injected the striatum of NT and R6/2 mice with AAV virus expressing either eGFP (as the control) or PIAS1 and performed complementary behavioral analyses as above. At 7 weeks, R6/2 mice overexpressing PIAS1 were not significantly different in Rotarod performance when compared to eGFP injected R6/2 controls (Figure 2F). R6/2 mice overexpressing PIAS1 demonstrated significantly impaired pole test descending times compared with eGFP treated R6/2 mice as early as 6 weeks of age (Figure 2G; Descending Time), with deficits disappearing at 8 weeks. For grip strength, R6/2 mice overexpressing PIAS1 were significantly weaker than eGFP injected mice at 8 weeks for grip strength task (Figure 2H). PIAS1 exacerbated the onset of clasping in R6/2 mice relative to eGFP treated mice (Figure 2I).

To determine whether PIAS1 modulation altered longevity in R6/2, we evaluated survival in a small cohort (n=5 for each condition) and found that PIAS1 knockdown significantly increased survival when compared to control, whereas PIAS1 overexpression HD mice had no significant effect (Figure S8A. Related to Figure 2).

Observational screens were performed weekly to rapidly assess general health, body weight, posture, appearance of the fur, neurological reflexes, home cage activity levels, and reactions to handling as designated by a multi-component Irwin Assessment Scale (Irwin, 1968). Of these parameters, modulation of PIAS1 appeared to show an effect on 3 physiological assessments: spontaneous activity, piloerection, and gait. Specifically, PIAS1 knockdown delayed the onset of abnormal spontaneous activity (Figure S8B. Related to Figure 2), piloerection (Figure S8C. Related to Figure 2), and gait impairments (Figure S8D. Related to Figure 2), relative to miSAFE and PIAS1 overexpression treated R6/2 mice. PIAS1 overexpression mice also exhibited earlier onset of abnormal physiological characteristics such as abnormal piloerection and gait impairments (Figure S8B–C. Related to Figure 2).

Taken together, these results demonstrate that PIAS1 knockdown significantly improves neurological phenotypes of R6/2 mice and that this effect is selective, given exacerbation of some phenotypes following PIAS1 overexpression. Interestingly, there were no significant differences across the battery of behavior assessments when comparing treatment effects on NT mice for either PIAS1 miRNA or cDNA delivery, supporting a selective role for PIAS1 in the disease setting.

PIAS1 knockdown decreases pathogenic accumulation of mHTT, SUMOylated, and Ubiquitinated proteins

Given that HMW mHTT species and SUMO-1 and 2/3 modified proteins accumulate in HD brain and that PIAS1 regulates accumulation of mHTT and SUMO-modified proteins in cells (O'Rourke et al., 2013), we investigated the impact of PIAS1 modulation on insoluble mHTT accumulation and protein homeostasis *in vivo*. The detergent insoluble fraction of R6/2 striatum plus and minus PIAS1 knockdown (mPIAS1.3 treatment) was analyzed for the presence of insoluble accumulated mHTT. Similar to our previous findings in cells, PIAS1 knockdown decreased insoluble HTT accumulation by ~60% in R6/2 mouse striatum (Figure 3A–B) compared to R6/2 treated with control virus (miSAFE). Further, this reduction in mHTT accumulation was due to PIAS1 knockdown and not to a decrease in mHTT transgene expression, as no differences in soluble mHTT transgene expression or HTT mRNA expression by RT-PCR between miPIAS1.3 treated mice compared to miSAFE were observed (Figure S5. Related to Figure 3).

We previously showed PIAS1 could modulate levels of SUMO-modified proteins in cells (O'Rourke et al., 2013) and here reduction of PIAS1 also significantly reduced levels of insoluble SUMO-1 (Figure 3A and 3C), SUMO-2 (Figure 3A and 3D), and ubiquitin-modified proteins (Figure 3A and 3E) in R6/2 striatum, suggesting that PIAS1 may be critical in generation of these modified and potentially pathogenic protein species. These fractions represent SUMO- and ubiquitin-modified cellular proteins including HTT as there are currently no antibodies that exclusively detect SUMO- or ubiquitin-modified HTT.

As observed for behavioral outcomes, overexpression of PIAS1 had the opposite effect compared to reduced PIAS1 and promoted aberrant protein accumulation and aggregation. Insoluble HTT accumulation was significantly increased in mouse striatum by week 9 (Figure 3F and 3H). Insoluble SUMO-1 (Figure 3F and 3H), SUMO-2 (Figure 3F and 3I),

and ubiquitin-modified proteins (Figure 3F and 3J) were also significantly increased in 9 week old R6/2 striatum following PIAS1 overexpression.

Finally, aberrant accumulation of mHTT is reflected in the formation of large visible aggregates, therefore we also evaluated the formation of inclusions in tissue sections from treated R6/2 mice. HTT-containing aggregates within the striatum were significantly reduced in striata of R6/2 mice injected with miPIAS1.3 compared to the miSAFE treated control group (Figure 4A). As expected, no inclusions were observed in NT mice (data not shown). Conversely, a 2-fold increase in inclusion bodies was observed in R6/2 mice treated with PIAS1 overexpressing vectors (Figure 4B).

Reduction of PIAS1 increases synaptophysin levels

A decrease in synaptic markers is associated with impaired synaptic activity and behavioral output in HD mice (Cepeda et al., 2003), whereas restoration of key synaptic marker levels prevented synapse degeneration, ameliorated motor and cognitive decline, and reduced striatal atrophy and neuronal loss in various mouse models of HD (Wang et al., 2014). Further, one of the many neural SUMOylation targets includes transporters and neurotransmitter receptors; factors critical to the health of a synapse (Sen and Snyder, 2010). Synaptophysin is a presynaptic marker that is decreased in the striatum of HD patients and animal models (Goto and Hirano, 1990); this decrease may be related to the accumulation of synaptotoxic mHTT species. Therefore we next investigated whether PIAS1 knockdown or overexpression modulates synaptophysin expression in R6/2 mice compared to controls, which may be an indication of overall synaptic health/function.

Immunohistochemical analysis of synaptophysin was performed on the striatum for both NT and R6/2 mice at 10 weeks for PIAS1 knockdown and 9 weeks for PIAS1 overexpression. Expression was quantified and significantly increased in striatal areas expressing miPIAS1.3 when compared to miSAFE in both HD and NT injected mice (Figure 5A; Figure S9. Related to Figure 5). In contrast, overexpression of PIAS1 resulted in a decrease of synaptophysin when compared to eGFP treated HD mice (Figure 5B), consistent with the increased HTT accumulation and worsening of behavioral readouts. There was no significant difference in synaptophysin levels in NT mice treated with either PIAS1 overexpression or eGFP control (Figure 5B).

Reduced PIAS1 selectively normalizes key dysregulated inflammatory markers in R6/2 mice

The PIAS1-SUMO ligase pathway plays a critical role in innate immune signaling and in inflammatory responses (Liu and Shuai, 2008; Liu et al., 2005). Importantly, these pathways are dysfunctional in HD (Shuai, 2006; Shuai and Liu, 2005). Chronic expression of mHTT results in sustained neuroinflammation which can cause elevated microglia activation and dysfunctional proinflammatory signaling, potentially contributing to neurotoxicity in HD. We evaluated whether altering PIAS1 levels in R6/2 striatum results in modulation of disease-associated neuroinflammation by investigating levels of key inflammatory proteins such as those expressed by activated microglia, inflammatory factors, and proinflammatory cytokines.

As microglia are intimately involved in regulation of inflammation, levels of anti-ionized calcium binding adaptor molecule 1 (Iba1), a marker for microglia in mouse tissue, was evaluated. Upon activation of microglia due to inflammation, expression of Iba1 is upregulated allowing the discrimination between surveying and activated microglia (Jeong et al., 2013). As expected, HD mice were found to have elevated steady-state levels of Iba1, consistent with increased neuroinflammation in the context of mHTT expression (Figures 6A and 6B). Treatment with miPIAS1.3 significantly reduced Iba1+ microglia (Figure 6A) within the virus-expressing regions, suggesting that mHTT accumulation and PIAS1 signaling may be essential for this neuroinflammatory effect. When PIAS1 was overexpressed, a significant increase in Iba1 protein staining was observed in HD mice (Figure 6B). Modulation of PIAS1 in NT mice did not yield a significant change in Iba1 levels compared to control treated mice (Figures 6A and 6B), suggesting that the presence of mHTT is an essential component of altered neuroinflammatory responses upon modulation of PIAS1.

Cytokines constitute a significant portion of the immuno- and neuromodulatory messengers that can be released by activated microglia. Additionally, PIAS1 regulates several downstream activators of pro-inflammatory cytokine signaling pathways including NF-κB (Shuai, 2006). We therefore examined NF-κB (p65) following modulation of PIAS1 in the insoluble striatal protein fraction which as shown above contains primarily nuclear and accumulated proteins. Consistent with previous studies (Camandola and Mattson, 2007), p65 levels were significantly decreased in the insoluble/nuclear fraction in R6/2, suggesting defective activation and localization of p65 to the nucleus (Figures 7A and 7B). Following PIAS1 knockdown in R6/2 mice, insoluble/nuclear p65 levels were increased and restored to NT levels (Figure 7A). In contrast, overexpression of PIAS1 did not alter p65 levels (Figure 7B).

Given Iba1 and NF-κB's role in inflammation, we next determined if changes in these markers corresponded to alterations in proinflammatory cytokines. We used a sensitive immunoassay panel to measure levels of IL1-β, IL-12p70, IFNγ, IL-6, IL-4, IL-5, IL-6, IL-2, KC/GRO, IL-10, and TNFα in striatal tissue. Several of these cytokines are altered in HD mouse models and human post-mortem tissue, including TNFα, IL1-β, IL-6, IL-10, and IFNγ (Ellrichmann et al., 2013; Silvestroni et al., 2009). Because detergent-insoluble samples contained high levels of SDS and can disrupt ELISA detection and that cytokines are soluble in nature, only soluble protein fractions were analyzed. Strikingly, PIAS1 reduction restored levels of several dysregulated proinflammatory cytokines back to NT levels. For instance, IL-6, and KC/GRO were significantly increased and IFNγ decreased in HD mice relative to NT animals (Figure 8A–D). However, this inflammatory effect was restored to NT levels in the presence of miPIAS1.3 (Figure 8A–C). In the case of IL1-β, HD mice have relatively high levels at baseline; PIAS1 knockdown increased its levels in controls and HD mice (Figure 8D). Further, there were no genotype or treatment effects for the other 7 cytokines on the panel (Figure S10B. Related to Figure 8), indicating selectivity in this PIAS1-mediated response for genes known to be dysregulated in HD systems and regulated by PIAS1 (Shuai, 2006). In contrast to PIAS1 reduction, PIAS1 overexpression did not elicit any changes to these same cytokines (e.g. IFNγ, IL-6, KC/GRO, IL1-β) in R6/2 mice (Figure 8E–H), possibly because PIAS1 levels are already high, or in NT controls. No

treatment effects were observed for striatal expression of the cytokines IL-12p70, IL-4, IL-5, IL-2, or IL-10 in NT or R6/2 animals, as with miPIAS1.3 (Figure S10B. Related to Figure 8).

These results suggest that PIAS1 knockdown results in the selective restoration of several inflammatory markers that are dysregulated in R6/2 mice and HD patients.

DISCUSSION

Approaches to reduce the causal entity in HD by targeting the production or accumulation of the mHTT protein itself are each likely to ameliorate HD pathogenesis. Here we describe a selective approach to reduce the accumulation of an insoluble, HMW and modified form of HTT *in vivo* in R6/2 mice through acute knockdown of the E3 SUMO ligase PIAS1, thereby reducing HD related phenotypes, significantly normalizing aberrant neuroinflammatory responses and potentially improving synaptic health in these mice. Outcomes were specific to preventing formation of this HTT species and to decreasing PIAS1 whereas overexpression of PIAS1 significantly exacerbated HD phenotypes and dysregulated protein homeostasis as measured by accumulation of pathogenic insoluble mHTT, SUMOylated, and ubiquitinated proteins.

PIAS1 and protein homeostasis

There is growing awareness that the SUMO network is important in a number of critical cellular processes, including pathways responsible for maintaining proteostasis through quality control, regulation of the turnover of cellular components, and stress responses. Age- and disease-related decline in protein homeostasis challenges the ability of neurons to counteract the accumulation of misfolded proteins. Their apparent critical role in regulating clearance of toxic mHTT clearance intermediates make SUMO and selective regulatory E3 ligases enticing targets for developing therapeutics for HD. Our findings indicate that PIAS1 may be a central feature in modulating the formation of accumulated/aggregated mHTT, either as a component of clearance mechanisms or through a contribution to the formation of toxic, modified clearance intermediates to be degraded. Our previous studies suggested that levels of PIAS1 can influence pathogenesis, given that reduced PIAS1 prevented aberrant accumulation of insoluble mHTT in cells (O'Rourke et al., 2013) and repressed PIAS1 was associated with improved behavior outcomes following AV.caRheb treatment in N171-82Q mice and WT control littermates (Lee et al., 2015). Importantly, PIAS1 appears to function at the protein homeostasis level versus acting to modulate HTT gene expression.

Post-translational modification of proteins such as tau, α-synuclein, and HTT has been linked to regulating their abundance in cells, potentially in association with cellular clearance networks (Pennuto et al., 2009; Popova et al., 2015). As protein clearance mechanisms become impaired upon aging, modified proteins which normally would be targeted for degradation may ultimately create accumulated clearance intermediates that take on toxic properties (Orr and Zoghbi, 2007; Shao and Diamond, 2007). The outcome is likely tied to the overall functional state of protein clearance pathways in the cell at a given time. For instance, SUMOylation of disease proteins can positively or negatively regulate aggregation potential and cellular homeostasis (Sarge and Park-Sarge, 2009). SUMOylated

proteins, as well as other post-translationally modified proteins, can act as clearance intermediates, effectively targeting them for degradation by either the UPS or by autophagy. However, when these pathways become blocked or impaired, proteins begin to accumulate and aggregate and further modification by ligases such as PIAS1 may generate more SUMOylated proteins than the system is able to effectively clear. It is possible that by reducing PIAS1 levels in our study, the formation of toxic HMW mHTT clearance intermediates is being significantly reduced, lightening the burden on the cell and shifting cellular homeostasis into a protective state.

PIAS1 and Neuroinflammation

In non-disease settings, inflammation acts as a homeostatic adaptive biological response to pathogen infection and tissue injury to activate the immune system and tissue repair mechanisms. However, when pathological processes result in a sustained inflammatory response, this chronic response may promote pathogenesis in several neurodegenerative diseases, including HD, and contribute to maladaptive responses that cause impaired neural plasticity and regeneration (Pekny and Pekna, 2014). Post-mortem human HD tissue has a distinct profile of inflammatory mediators such as increased gene expression of IL1-β, IL-8 (*KC/GRO in mice*), IL-6, and TNFα in the cortex and cerebellum (Silvestroni et al., 2009), decreased IL1-β, IL-8, TNFα and increased IL-6 mRNA levels in both human HD and R6/2 mouse striatum (Laprairie et al., 2014). How these mediators contribute to disease is unclear.

We investigated the protein expression of key inflammatory mediators in the presence of PIAS1 modulation and observe selective restoration of inflammatory signaling. First, although TNFα levels are higher in the plasma and brain tissues of mice and patients with HD (Bjorkqvist et al., 2008), PIAS1 modulation did not appear to impact TNFα levels, suggesting that PIAS1's effects on cytokine and inflammatory state may be downstream of TNFα regulation, potentially at the level of NF-κB. HTT can interact with p65 and mHTT expression impairs transport of NF-κB from the synapse to the nucleus, a process which appears to be critical to cell survival, synaptic plasticity, and neuroprotection (Marcora and Kennedy, 2010). Inappropriate regulation of NF-κB is involved in a wide range of neurodegenerative disorders including HD (Camandola and Mattson, 2007) and p65 activation normalizes the expression of several cytokine genes in HD models (Laprairie et al., 2014). PIAS1 is an important negative regulator of NF-κB transcription factors that are activated by proinflammatory cytokines, growth factors, bacterial lipopolysaccharides, viruses, and stress signals (Liu et al., 2005). The binding of PIAS1 to p65 inhibits cytokine-induced NF-κB-dependent gene activation and induction of proinflammatory cytokine transcription, predicting that decreasing PIAS1 could restore NF-κB activity. Indeed, reduction of PIAS1 restored insoluble/nuclear p65 to NT levels (Figure 6C). An intriguing connection between protein accumulation and these inflammatory responses is that IκB kinase β can regulate p65 clearance; this kinase also phosphorylates HTT S13 (Khoshnan and Patterson, 2011; Oeckinghaus and Ghosh, 2009; Thompson et al., 2009), which both facilitates SUMO modification of HTT and clearance of mHTT. It is conceivable that PIAS1 is involved in this regulatory loop.

Levels of microglia are also decreased following PIAS1 knockdown in R6/2 mice (Figure 6A). Microglial activation is observed in R6/2 mice and HD human tissue (Simmons et al., 2007) and expression of mHTT in microglia is sufficient to activate microglia and induce inflammatory responses via the myeloid lineage-determining factors PU.1 and C/EBPs (Crotti et al., 2014). Remarkably, PIAS1 serves as a SUMO E3 ligase to regulate C/EBPβ activity (Liu et al., 2013) suggesting PIAS1 may be critical to this pathway which is dysfunctional in HD. Given that cellular debris from degenerating neurons, including aggregates, can stimulate inflammatory cascades by microglia (Eyo and Wu, 2013; Suzumura, 2013), the prevention of mHTT accumulation may directly influence microglial activation. Indeed, we find that specific modulation of PIAS1 in neurons (Figure 1B–C) may alter cell-to-cell communication with neighboring glial cells to alter inflammatory homeostasis. One powerful aspect of this study comes from comparing the behavioral and neuropathological changes to mHTT proteostasis and inflammatory markers, which allows predictions as to the relevance of each that can be formally tested in future studies. A potential association between effects on HTT proteostasis is that microglial neuronal toxicity may account for loss of synaptophysin (Rasmussen et al., 2007), therefore by reducing levels of Iba1, and possibly activated microglia, PIAS1 knockdown may indirectly restore levels of synaptophysin in response to reduced neuronal toxicity. The significant reduction of accumulated insoluble mHTT and modified proteins in cells may restore positive cell-to-cell signaling between transduced neurons and neighboring/recruited microglia to limit the progression of a disease inflammatory state. PIAS1 knockdown, however, also appears to elicit selective effects beyond reducing mHTT accumulation. For instance, synaptophysin levels were increased in both NT and HD lines at 10 weeks following PIAS1 knockdown, suggesting that synaptotoxicity could be reversed both as a consequence of reduced mHTT accumulation but also at least in part, directly as a consequence of PIAS1 activity.

PIAS1 is critically involved in the regulation of several key inflammatory signaling nodes (Liu et al., 2007; Shuai, 2006; Shuai and Liu, 2005) including STAT1, NF-κB as mentioned, and interferon-inducible genes and PIAS1 can negatively regulate interferon-inducible genes (Shuai, 2006). When interferon pathways are activated, clearance of accumulated misfolded proteins is induced and cytotoxicity reduced in HD (Lu et al., 2013), SCA (Chort et al., 2013) and ALS (Hadano et al., 2010) models. IFN-γ levels are increased following PIAS1 knockdown in R6/2, consistent with PIAS1's role as a negative regulator for IFN-γ mediated innate immune responses (Liu et al., 2004). As many of these highly relevant networks are transcriptionally regulated by PIAS, PIAS1 may therefore play a fundamental role in HD pathogenesis through a combined impact on SUMO modification pathways and transcriptional networks. Consistent with our findings, PIAS1-homozygous null mice have elevated proinflammatory cytokine IL1-β levels relative to their wild type littermates (Liu et al., 2007).

R6/2 mouse model and next steps

Based on findings presented here using a rapidly progressing mouse model, R6/2, that expresses an amino terminal fragment of the full length mHTT protein (Mangiarini et al., 1996), PIAS1 knockdown would be predicted to be neuroprotective and potentially effective when treatment is initiated symptomatically or early in disease. However, this likely depends

on model and/or disease stage. Pathogenesis in R6/2 mice represents aspects of manifest HD, showing demonstrable protein accumulation, nuclear HTT localization, neuroinflammation, and dysregulated transcriptional signatures similar to striatal tissues from both symptomatic full length knock-in mouse models of disease and to human HD brain (Chang et al., 2015; Ciamei et al., 2015; Simmons et al., 2007). It will be essential to evaluate the effects of PIAS1 modulation in full length models of HD at various stages of the disease and perhaps in human patient-derived induced pluripotent stem cell neuronal subtypes in future studies in order to fully understand the contribution of PIAS1 to disease and its potential as a clinical target. Further, our findings elucidate effects on neuronal dysfunction versus neurodegenerative aspects of disease, given the limited neuronal loss that is observed in mouse models of HD relative to human HD.

Summary

There is immense molecular complexity of inflammatory responses in HD. The data suggests that PIAS1 may link protein homeostasis and neuroinflammation in HD through a combination of modulating or compensating for dysfunctional inflammatory signaling cascades between neurons and microglia, and modulating accumulation of toxic HMW species of HTT, potentially allowing improved flux through protein clearance pathways. Given that PIAS proteins regulate several critical cellular processes, such as transcription, immune responses, and cytokine signaling (Liu and Shuai, 2008; Rytinki et al., 2009), and the likelihood that these processes play critical roles in different stages of disease and development, PIAS1 may thus serve as an “opportunistic” target. As a therapeutic target, homozygous animals display partial perinatal lethality (Shuai, 2006), suggesting a requirement for sufficient PIAS1 during development, however heterozygous null mice do not display any perinatal lethality and are clinically normal. Of significance, no deleterious effects were observed in NT animals following partial reduction of PIAS1, suggesting that a therapeutic reduction of PIAS1 could be safe through knockdown or small molecule inhibitors. PIAS1 protein levels were not significantly altered in these NT mice, despite expression of AAVs and decreased mRNA levels (Figure S5. Related to Figure 1). It is possible that other PIAS proteins and/or overall cellular homeostasis mechanisms may normally maintain PIAS1 levels under strict control by either clearing out excess or maintaining levels of PIAS1 when overexpressed or knocked down. Supporting this concept is the presence of a C-terminal domain responsible for targeting for PIAS1 for proteolysis/clearance (Reindle et al., 2006). These cellular processes may be less functional in the expanded polyglutamine repeat context, as highlighted by the accumulation of PIAS1 in HD mice and impact on this accumulation through exogenous targeting of expression. The fundamental properties identified here may also broadly impact other neurodegeneration diseases, suggesting that PIAS1 and other E3 SUMO ligases may be key to tipping the balance between normal protein homeostasis and disease processes that cause neurodegeneration.

EXPERIMENTAL PROCEDURES

Animals

Experiments were carried out in strict accordance with the Guide for the Care and Use of Laboratory Animals of the National Institutes of Health and an approved animal research protocol by the Institutional Animal Care and Use Committee (IACUC) at the University of California, Irvine, an AAALAC accredited institution. All efforts were made to minimize animal suffering. R6/2 mice were obtained from Jackson Laboratories (Bar Harbor, ME) (RRID:IMSR_JAX:006494) and housed under 12 h light/dark cycle in groups of up to 5 animals/cage with food and water ad libitum. CAG repeat sizing of tails and a subset of striatal tissue was performed (Laragen, Los Angeles, CA). To justify group and trial sizes in the animal experiments, we used G Power (http://www.psycho.uni-duesseldorf.de/abteilungen/aap/gpower3/). Assessment of differences in outcome were based upon our previous experience and published results (Carter et al., 1999; Hickey et al., 2005; Hockly et al., 2003; Stack et al., 2005). Applying the power analysis to analysis of variance model under these conditions and assumptions we arrived at an n=10 per experiment for behavior and n=4 for biochemical analysis.

Injections

Bilateral intrastriatal injections were performed using a stereotaxic apparatus (coordinates 0.01mm caudal to bregma, 0.2mm right/left of midline, 0.345 pocket to 0.325mm ventral to pial surface). Mice were anesthetized with isofluorane, placed in the stereotax and 5μl (~3e12vg/ml) of either vector was dispensed in each hemisphere's striatum with a Hamilton syringe (Hamilton, Reno, NV). Animals were injected with ~ 3e12vg/ml of either rAAV2/1mU6miSAFECMVeGFP (n=10), rAAV2/1mU6miPIAS1.3CMVeGFP (n=10), rAAV2/2CMVeGFP (n=10), or rAV2/2CMVPIAS1 (n=10) at a rate of 0.5μl/min and the needle was left in place for 2 min after each injection. Once completed, the incision was sutured.

Behavior and Tissue Collection for Biochemical Processing

Behavioral studies were performed one week following surgeries and analyzed blinded using Rotarod, pole test, grip strength, and Irwin assessment (Supplemental Experimental Procedures). Mice were sacrificed by Euthasol and transcardial perfusion. For biochemical assessment, cortex, striatum, and cerebellum was microdissected from flash-frozen half brains and stored at −80C until processing; 40μm sections of post-fixed half brains were processed for immunohistochemistry and imaged via confocal microscopy. All animals were assigned to treatment groups with randomly generated identification codes to keep the researcher blinded throughout testing and analysis.

Immunohistochemistry and Quantitation

The following primary antibodies were used: anti-Iba1 (Wako Cat# 27030 RRID:AB_2314667), anti-GFAP (Abcam Cat# ab7260 RRID:AB_305808), anti-HTT (X.J. Li, Emory University School of Medicine; Georgia; USA Cat# mEM48 RRID:AB_2307353), anti-Synaptophysin (Sigma-Aldrich Cat# S5768 RRID:AB_477523),

and anti-βIII Tubulin (Covance Research Products Inc Cat# PRB-435P-100 RRID:AB_10063850). Alexa fluorescent conjugated secondary antibodies were used (Innovative Research Cat# A21103 RRID:AB_1500591, Thermo Fisher Scientific Cat# A21050 RRID:AB_10562369, Thermo Fisher Scientific Cat# A21070 RRID:AB_10562894, Thermo Fisher Scientific Cat# A21428 RRID:AB_10561552, Thermo Fisher Scientific Cat# A21422 RRID:AB_10561696). Stained tissue was mounted on slides and cover slipped with Fluoromount-G (SouthernBiotech). Images were acquired on a LeicaDM2500 confocal microscope. For each brain, five representative sections were chosen and eGFP localized 10x, 20x, and 63x z-stack images obtained for each treatment using confocal microscopy at comparable sections in each animal. Stacked images were obtained for each section containing viral expression as reported by eGFP expression, followed by automatic analyses using Imaris Bitplane 5.0.

Western Blot Analysis

Whole mouse striatum tissue was processed for either soluble/insoluble fractionation as previously described (O'Rourke et al., 2013) (Supplemental Experimental Procedures) or with TPER buffer with protease inhibitors (Complete Mini, Roche Applied Science, Mannheim) and phosphatase inhibitors (PhosSTOP Phosphatase Inhibitor Cocktail, Roche Applied Science, Mannheim). Protein concentration was determined by BCA assay (Pierce, Rockford), and 30μg of protein was reduced, loaded on 3–8% bis-acrylamide gels/4%–12% bis-tris mini gels (Life Technologies) for SDS-PAGE, transferred to nitrocellulose membrane, and nonspecific proteins were blocked with SuperBlock Blocking Buffer (Thermo Scientific). Primary antibodies used were: Anti-HTT (Millipore Cat# MAB5492 RRID:AB_347723); Anti-HTT (VIVA Bioscience Cat# VB3130, RRID:AB_2566818); Living Colors Full-Length Antibody (Clontech Laboratories, Inc. Cat# 632381 RRID:AB_2313808); anti-mPIAS1 (Thermo Fisher Scientific Cat# 396600 RRID:AB_10151462); anti-SUMO-1 (Enzo Life Sciences Cat# BML-PW9460 RRID:AB_10542961), anti-SUMO-2 (MBL International Cat# M114-A48 RRID:AB_1953063); anti-Ubiquitin (Santa Cruz Biotechnology Cat# sc-8017 RRID:AB_628423); anti-NFκB p65 (Santa Cruz Biotechnology Cat# sc-8008 RRID:AB_628017), anti-Histone H3 (Millipore Cat# 06-755 RRID:AB_2118461), anti-GAPDH (IMGENEX Cat# IMG-5019A-1 RRID:AB_316884), and anti-α-tubulin (Sigma-Aldrich Cat# T6074 RRID:AB_477582). Blots were developed using Pico/Dura Western Blotting Detection System (Pierce) and exposed to film for images. Protein quantification was performed using Scion Image analysis software. Band densities were normalized to α-tubulin.

RNA Isolation and Real-Time Quantitative PCR

Brain tissues were homogenized in TRIzol (Invitrogen), and total RNA was isolated using RNEasy Mini kit (QIAGEN). DNase treatment was incorporated into the RNEasy procedure in order to remove residual DNA. RIN values were >9 for each sample (Agilent Bioanalyzer). Reverse transcription was performed using oligo dT primers and 1μg of total RNA using SuperScript III First-Strand Synthesis System (Invitrogen). Quantitative PCR was performed as previously described (Vashishtha et al., 2013) and ddCT values were quantitated and analyzed against RPLPO.

Statistical analysis

Statistical analyses were performed using GraphPad Prism 5.04 software. All data are expressed as mean ± SEM, and a value of $p<0.05$ was considered to be statistically significant. Statistical comparisons of densitometry results were performed by one-way ANOVA followed by Bonferroni's multiple comparison tests. Student's t tests were used for aggregate size and number comparisons from the EM48 immuno-labeling study. One-way ANOVA followed by Bonferroni's multiple comparison tests was used to establish significance of the body weight analysis from the R6/2 mouse study. Significance in the clasping assay was determined by Fisher's exact probability test. The Rotarod and pole test data were analyzed by one-way ANOVA followed by Bonferroni's multiple comparisons tests.

Supplementary Material

Refer to Web version on PubMed Central for supplementary material.

Acknowledgments

This work was supported by grants from the National Institute of Health (NS090390 to LMT and BD, NS52789 to LMT, NS072453 to JSS, NS076631 to BLD). Support was also provided by the Hereditary Disease Foundation (JSS and Leslie Gehry Brenner prize to LMT), CHDI Foundation (JSS), The Roy J Carver Trust and The Children's Hospital of Philadelphia Research Institute (BLD), Hoppy's Hope Foundation (AMM), the Janet Westerfield Foundation (to JO), and NSF fellowship (to JO). We would like to thank Eva Morozko, Sylvia Yeung, and Alice Lau for technical assistance, David E. Housman (MIT) and Ignacio Munoz-Sanjuan (CHDI) for helpful discussions. We also would like to thank the UCI Institute for Memory Impairments and Neurological Disorders and the Optical Biology Shared Resource of the Cancer Center Support Grant (CA-62203) at the University of California, Irvine for assistance in carrying out experiments.

References

Aschauer DF, Kreuz S, Rumpel S. Analysis of transduction efficiency, tropism and axonal transport of AAV serotypes 1, 2, 5, 6, 8 and 9 in the mouse brain. PloS one. 2013; 8:e76310. [PubMed: 24086725]

Bjorkqvist M, Wild EJ, Thiele J, Silvestroni A, Andre R, Lahiri N, Raibon E, Lee RV, Benn CL, Soulet D, et al. A novel pathogenic pathway of immune activation detectable before clinical onset in Huntington's disease. The Journal of experimental medicine. 2008; 205:1869–1877. [PubMed: 18625748]

Camandola S, Mattson MP. NF-kappa B as a therapeutic target in neurodegenerative diseases. Expert Opin Ther Targets. 2007; 11:123–132. [PubMed: 17227229]

Carter RJ, Lione LA, Humby T, Mangiarini L, Mahal A, Bates GP, Dunnett SB, Morton AJ. Characterization of progressive motor deficits in mice transgenic for the human Huntington's disease mutation. J Neurosci. 1999; 19:3248–3257. [PubMed: 10191337]

Cepeda C, Hurst RS, Calvert CR, Hernandez-Echeagaray E, Nguyen OK, Jocoy E, Christian LJ, Ariano MA, Levine MS. Transient and progressive electrophysiological alterations in the corticostriatal pathway in a mouse model of Huntington's disease. J Neurosci. 2003; 23:961–969. [PubMed: 12574425]

Chang KH, Wu YR, Chen YC, Chen CM. Plasma inflammatory biomarkers for Huntington's disease patients and mouse model. Brain Behav Immun. 2015; 44:121–127. [PubMed: 25266150]

Chort A, Alves S, Marinello M, Dufresnois B, Dornbierer JG, Tesson C, Latouche M, Baker DP, Barkats M, El Hachimi KH, et al. Interferon beta induces clearance of mutant ataxin 7 and improves locomotion in SCA7 knock-in mice. Brain. 2013; 136:1732–1745. [PubMed: 23518714]

Ciamei A, Detloff PJ, Morton AJ. Progression of behavioural despair in R6/2 and Hdh knock-in mouse models recapitulates depression in Huntington's disease. Behav Brain Res. 2015; 291:140–146. [PubMed: 25986402]

Crotti A, Benner C, Kerman BE, Gosselin D, Lagier-Tourenne C, Zuccato C, Cattaneo E, Gage FH, Cleveland DW, Glass CK. Mutant Huntingtin promotes autonomous microglia activation via myeloid lineage-determining factors. Nature neuroscience. 2014; 17:513–521. [PubMed: 24584051]

Cubenas-Potts C, Matunis MJ. SUMO: a multifaceted modifier of chromatin structure and function. Developmental cell. 2013; 24:1–12. [PubMed: 23328396]

Datwyler AL, Lattig-Tunnemann G, Yang W, Paschen W, Lee SL, Dirnagl U, Endres M, Harms C. SUMO2/3 conjugation is an endogenous neuroprotective mechanism. Journal of cerebral blood flow and metabolism: official journal of the International Society of Cerebral Blood Flow and Metabolism. 2011; 31:2152–2159.

Ehrnhoefer DE, Sutton L, Hayden MR. Small changes, big impact: posttranslational modifications and function of huntingtin in Huntington disease. The Neuroscientist: a review journal bringing neurobiology, neurology and psychiatry. 2011; 17:475–492.

Ellrichmann G, Reick C, Saft C, Linker RA. The role of the immune system in Huntington's disease. Clin Dev Immunol. 2013; 2013:541259. [PubMed: 23956761]

Eyo UB, Wu LJ. Bidirectional microglia-neuron communication in the healthy brain. Neural plasticity. 2013; 2013:456857. [PubMed: 24078884]

Gareau JR, Lima CD. The SUMO pathway: emerging mechanisms that shape specificity, conjugation and recognition. Nat Rev Mol Cell Biol. 2010; 11:861–871. [PubMed: 21102611]

Goto S, Hirano A. Synaptophysin expression in the striatum in Huntington's disease. Acta Neuropathol. 1990; 80:88–91. [PubMed: 2141751]

The Huntington's Disease Collaborative Research Group. A novel gene containing a trinucleotide repeat that is expanded and unstable on Huntington's disease chromosomes. Cell. 1993; 72:971–983. [PubMed: 8458085]

Gu X, Li C, Wei W, Lo V, Gong S, Li SH, Iwasato T, Itohara S, Li XJ, Mody I, et al. Pathological cell-cell interactions elicited by a neuropathogenic form of mutant Huntingtin contribute to cortical pathogenesis in HD mice. Neuron. 2005; 46:433–444. [PubMed: 15882643]

Hadano S, Otomo A, Kunita R, Suzuki-Utsunomiya K, Akatsuka A, Koike M, Aoki M, Uchiyama Y, Itoyama Y, Ikeda JE. Loss of ALS2/Alsin exacerbates motor dysfunction in a SOD1-expressing mouse ALS model by disturbing endolysosomal trafficking. PloS one. 2010; 5:e9805. [PubMed: 20339559]

Harper SQ, Staber PD, He X, Eliason SL, Martins IH, Mao Q, Yang L, Kotin RM, Paulson HL, Davidson BL. RNA interference improves motor and neuropathological abnormalities in a Huntington's disease mouse model. Proc Natl Acad Sci U S A. 2005; 102:5820–5825. [PubMed: 15811941]

Hickey MA, Gallant K, Gross GG, Levine MS, Chesselet MF. Early behavioral deficits in R6/2 mice suitable for use in preclinical drug testing. Neurobiol Dis. 2005; 20:1–11. [PubMed: 16137562]

Hickey MA, Kosmalska A, Enayati J, Cohen R, Zeitlin S, Levine MS, Chesselet MF. Extensive early motor and non-motor behavioral deficits are followed by striatal neuronal loss in knock-in Huntington's disease mice. Neuroscience. 2008; 157:280–295. [PubMed: 18805465]

Hockly E, Woodman B, Mahal A, Lewis CM, Bates G. Standardization and statistical approaches to therapeutic trials in the R6/2 mouse. Brain Res Bull. 2003; 61:469–479. [PubMed: 13679245]

Hsiao HY, Chen YC, Chen HM, Tu PH, Chern Y. A critical role of astrocyte-mediated nuclear factor-kappaB-dependent inflammation in Huntington's disease. Hum Mol Genet. 2013; 22:1826–1842. [PubMed: 23372043]

Irwin S. Comprehensive observational assessment: Ia. A systematic, quantitative procedure for assessing the behavioral and physiologic state of the mouse. Psychopharmacologia. 1968; 13:222–257. [PubMed: 5679627]

Jeong HK, Ji K, Min K, Joe EH. Brain inflammation and microglia: facts and misconceptions. Exp Neurobiol. 2013; 22:59–67. [PubMed: 23833554]

Khoshnan A, Patterson PH. The role of IkappaB kinase complex in the neurobiology of Huntington's disease. Neurobiol Dis. 2011; 43:305–311. [PubMed: 21554955]

Krumova P, Weishaupt JH. Sumoylation in neurodegenerative diseases. Cellular and molecular life sciences: CMLS. 2013; 70:2123–2138. [PubMed: 23007842]

La Spada AR, Taylor JP. Repeat expansion disease: progress and puzzles in disease pathogenesis. Nature reviews Genetics. 2010; 11:247–258.

Laprairie RB, Warford JR, Hutchings S, Robertson GS, Kelly ME, Denovan-Wright EM. The cytokine and endocannabinoid systems are co-regulated by NF-kappaB p65/RelA in cell culture and transgenic mouse models of Huntington's disease and in striatal tissue from Huntington's disease patients. Journal of neuroimmunology. 2014; 267:61–72. [PubMed: 24360910]

Lee JH, Park SM, Kim OS, Lee CS, Woo JH, Park SJ, Joe EH, Jou I. Differential SUMOylation of LXRalpha and LXRbeta mediates transrepression of STAT1 inflammatory signaling in IFN-gamma-stimulated brain astrocytes. Molecular cell. 2009; 35:806–817. [PubMed: 19782030]

Lee JH, Tecedor L, Chen YH, Monteys AM, Sowada MJ, Thompson LM, Davidson BL. Reinstating aberrant mTORC1 activity in Huntington's disease mice improves disease phenotypes. Neuron. 2015; 85:303–315. [PubMed: 25556834]

Liu B, Mink S, Wong KA, Stein N, Getman C, Dempsey PW, Wu H, Shuai K. PIAS1 selectively inhibits interferon-inducible genes and is important in innate immunity. Nat Immunol. 2004; 5:891–898. [PubMed: 15311277]

Liu B, Shuai K. Targeting the PIAS1 SUMO ligase pathway to control inflammation. Trends in pharmacological sciences. 2008; 29:505–509. [PubMed: 18755518]

Liu B, Shuai K. Summon SUMO to wrestle with inflammation. Molecular cell. 2009; 35:731–732. [PubMed: 19782020]

Liu B, Yang R, Wong KA, Getman C, Stein N, Teitell MA, Cheng G, Wu H, Shuai K. Negative regulation of NF-kappaB signaling by PIAS1. Molecular and cellular biology. 2005; 25:1113–1123. [PubMed: 15657437]

Liu B, Yang Y, Chernishof V, Loo RR, Jang H, Tahk S, Yang R, Mink S, Shultz D, Bellone CJ, et al. Proinflammatory stimuli induce IKKalpha-mediated phosphorylation of PIAS1 to restrict inflammation and immunity. Cell. 2007; 129:903–914. [PubMed: 17540171]

Liu Y, Zhang YD, Guo L, Huang HY, Zhu H, Huang JX, Liu Y, Zhou SR, Dang YJ, Li X, et al. Protein inhibitor of activated STAT 1 (PIAS1) is identified as the SUMO E3 ligase of CCAAT/enhancer-binding protein beta (C/EBPbeta) during adipogenesis. Molecular and cellular biology. 2013; 33:4606–4617. [PubMed: 24061474]

Lu B, Al-Ramahi I, Valencia A, Wang Q, Berenshteyn F, Yang H, Gallego-Flores T, Ichcho S, Lacoste A, Hild M, et al. Identification of NUB1 as a suppressor of mutant Huntington toxicity via enhanced protein clearance. Nature neuroscience. 2013; 16:562–570. [PubMed: 23525043]

Mangiarini L, Sathasivam K, Seller M, Cozens B, Harper A, Hetherington C, Lawton M, Trottier Y, Lehrach H, Davies SW, et al. Exon 1 of the HD gene with an expanded CAG repeat is sufficient to cause a progressive neurological phenotype in transgenic mice. Cell. 1996; 87:493–506. [PubMed: 8898202]

Marcora E, Kennedy MB. The Huntington's disease mutation impairs Huntingtin's role in the transport of NF-kappaB from the synapse to the nucleus. Hum Mol Genet. 2010; 19:4373–4384. [PubMed: 20739295]

McBride JL, Boudreau RL, Harper SQ, Staber PD, Monteys AM, Martins I, Gilmore BL, Burstein H, Peluso RW, Polisky B, et al. Artificial miRNAs mitigate shRNA-mediated toxicity in the brain: implications for the therapeutic development of RNAi. Proc Natl Acad Sci U S A. 2008; 105:5868–5873. [PubMed: 18398004]

O'Rourke JG, Gareau JR, Ochaba J, Song W, Rasko T, Reverter D, Lee J, Monteys AM, Pallos J, Mee L, et al. SUMO-2 and PIAS1 modulate insoluble mutant huntingtin protein accumulation. Cell reports. 2013; 4:362–375. [PubMed: 23871671]

Oeckinghaus A, Ghosh S. The NF-kappaB family of transcription factors and its regulation. Cold Spring Harb Perspect Biol. 2009; 1:a000034. [PubMed: 20066092]

Orr HT, Zoghbi HY. Trinucleotide repeat disorders. Annu Rev Neurosci. 2007; 30:575–621. [PubMed: 17417937]

Pekny M, Pekna M. Astrocyte reactivity and reactive astrogliosis: costs and benefits. Physiological reviews. 2014; 94:1077–1098. [PubMed: 25287860]

Pennuto M, Palazzolo I, Poletti A. Post-translational modifications of expanded polyglutamine proteins: impact on neurotoxicity. Hum Mol Genet. 2009; 18:R40–47. [PubMed: 19297400]

Popova B, Kleinknecht A, Braus GH. Posttranslational Modifications and Clearing of alpha-Synuclein Aggregates in Yeast. Biomolecules. 2015; 5:617–634. [PubMed: 25915624]

Praefcke GJ, Hofmann K, Dohmen RJ. SUMO playing tag with ubiquitin. Trends in biochemical sciences. 2012; 37:23–31. [PubMed: 22018829]

Rasmussen S, Wang Y, Kivisakk P, Bronson RT, Meyer M, Imitola J, Khoury SJ. Persistent activation of microglia is associated with neuronal dysfunction of callosal projecting pathways and multiple sclerosis-like lesions in relapsing--remitting experimental autoimmune encephalomyelitis. Brain. 2007; 130:2816–2829. [PubMed: 17890734]

Reindle A, Belichenko I, Bylebyl GR, Chen XL, Gandhi N, Johnson ES. Multiple domains in Siz SUMO ligases contribute to substrate selectivity. J Cell Sci. 2006; 119:4749–4757. [PubMed: 17077124]

Ross CA, Tabrizi SJ. Huntington's disease: from molecular pathogenesis to clinical treatment. Lancet neurology. 2011; 10:83–98. [PubMed: 21163446]

Rytinki MM, Kaikkonen S, Pehkonen P, Jaaskelainen T, Palvimo JJ. PIAS proteins: pleiotropic interactors associated with SUMO. Cellular and molecular life sciences: CMLS. 2009; 66:3029–3041. [PubMed: 19526197]

Sarge KD, Park-Sarge OK. Sumoylation and human disease pathogenesis. Trends in biochemical sciences. 2009; 34:200–205. [PubMed: 19282183]

Sen N, Snyder SH. Protein modifications involved in neurotransmitter and gasotransmitter signaling. Trends Neurosci. 2010; 33:493–502. [PubMed: 20843563]

Shao J, Diamond MI. Polyglutamine diseases: emerging concepts in pathogenesis and therapy. Hum Mol Genet. 2007; 16(Spec No 2):R115–123. [PubMed: 17911155]

Shuai K. Regulation of cytokine signaling pathways by PIAS proteins. Cell research. 2006; 16:196–202. [PubMed: 16474434]

Shuai K, Liu B. Regulation of gene-activation pathways by PIAS proteins in the immune system. Nat Rev Immunol. 2005; 5:593–605. [PubMed: 16056253]

Silvestroni A, Faull RL, Strand AD, Moller T. Distinct neuroinflammatory profile in postmortem human Huntington's disease. Neuroreport. 2009; 20:1098–1103. [PubMed: 19590393]

Simmons DA, Casale M, Alcon B, Pham N, Narayan N, Lynch G. Ferritin accumulation in dystrophic microglia is an early event in the development of Huntington's disease. Glia. 2007; 55:1074–1084. [PubMed: 17551926]

Sontag EM, Lotz GP, Yang G, Sontag CJ, Cummings BJ, Glabe CG, Muchowski PJ, Thompson LM. Detection of Mutant Huntingtin Aggregation Conformers and Modulation of SDS-Soluble Fibrillar Oligomers by Small Molecules. J Huntingtons Dis. 2012; 1:127–140.

Stack EC, Kubilus JK, Smith K, Cormier K, Del Signore SJ, Guelin E, Ryu H, Hersch SM, Ferrante RJ. Chronology of behavioral symptoms and neuropathological sequela in R6/2 Huntington's disease transgenic mice. J Comp Neurol. 2005; 490:354–370. [PubMed: 16127709]

Steffan JS, Agrawal N, Pallos J, Rockabrand E, Trotman LC, Slepko N, Illes K, Lukacsovich T, Zhu YZ, Cattaneo E, et al. SUMO modification of Huntingtin and Huntington's disease pathology. Science. 2004; 304:100–104. [PubMed: 15064418]

Suzumura A. Neuron-microglia interaction in neuroinflammation. Current protein & peptide science. 2013; 14:16–20. [PubMed: 23544747]

Thompson LM, Aiken CT, Kaltenbach LS, Agrawal N, Illes K, Khoshnan A, Martinez-Vincente M, Arrasate M, O'Rourke JG, Khashwji H, et al. IKK phosphorylates Huntingtin and targets it for degradation by the proteasome and lysosome. The Journal of cell biology. 2009; 187:1083–1099. [PubMed: 20026656]

Vashishtha M, Ng CW, Yildirim F, Gipson TA, Kratter IH, Bodai L, Song W, Lau A, Labadorf A, Vogel-Ciernia A, et al. Targeting H3K4 trimethylation in Huntington disease. Proc Natl Acad Sci U S A. 2013; 110:E3027–3036. [PubMed: 23872847]

Waelter S, Boeddrich A, Lurz R, Scherzinger E, Lueder G, Lehrach H, Wanker EE. Accumulation of mutant huntingtin fragments in aggresome-like inclusion bodies as a result of insufficient protein degradation. Molecular biology of the cell. 2001; 12:1393–1407. [PubMed: 11359930]

Wang N, Gray M, Lu XH, Cantle JP, Holley SM, Greiner E, Gu X, Shirasaki D, Cepeda C, Li Y, et al. Neuronal targets for reducing mutant huntingtin expression to ameliorate disease in a mouse model of Huntington's disease. Nat Med. 2014; 20:536–541. [PubMed: 24784230]

Wilkinson KA, Nakamura Y, Henley JM. Targets and consequences of protein SUMOylation in neurons. Brain research reviews. 2010; 64:195–212. [PubMed: 20382182]

Woodman B, Butler R, Landles C, Lupton MK, Tse J, Hockly E, Moffitt H, Sathasivam K, Bates GP. The Hdh(Q150/Q150) knock-in mouse model of HD and the R6/2 exon 1 model develop comparable and widespread molecular phenotypes. Brain Res Bull. 2007; 72:83–97. [PubMed: 17352931]

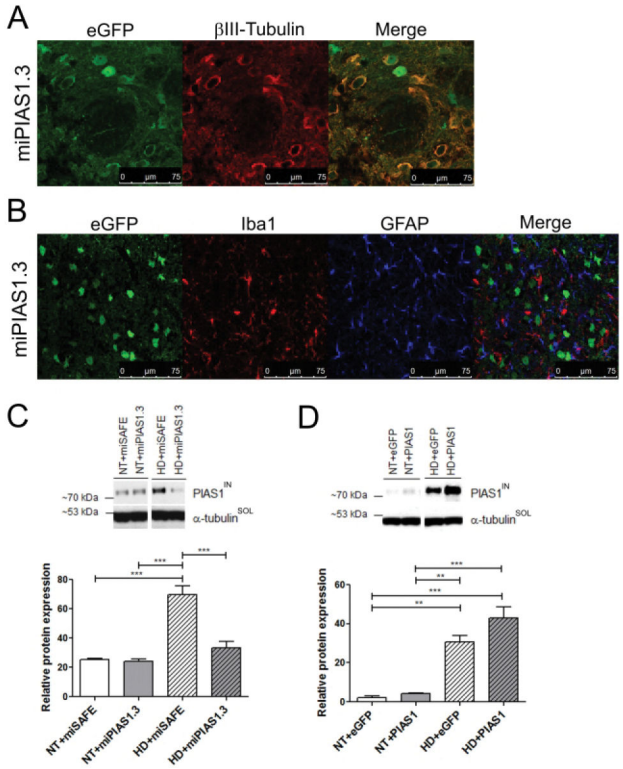

Figure 1. PIAS1 levels are modulated in R6/2 mouse model following viral-mediated knockdown or overexpression

(A–B) miPIAS1.3 viral expression is limited to neurons. Confocal images of R6/2 striatum (63x) with miPIAS1.3. (A) Red: immunohistochemical label for βIII-Tubulin, a neuronal marker; green: GFP expression of viral vector. (B) Red: immunohistochemical label for Iba1, a microglia marker; blue: GFAP, an astrocyte marker; green: GFP expression of viral vector. Scale bar = 75 μm. (C) Immunoblotting of PIAS1 from 10-week-old R6/2 and NT mouse striatal lysates following viral mediated miSAFE or miPIAS1.3 treatment. Insoluble PIAS1 levels are significantly reduced following miPIAS1.3 treatment in R6/2, but not NT mice compared to eGFP treatment. All data are expressed as western quantitation and relative expression to NT + miSAFE treated mice. Protein expression was validated for protein loading prior to antibody incubation using reversible protein stain and each samples' corresponding soluble α-tubulin expression. (D) Immunoblotting of PIAS1 from 9-week-old R6/2 and NT mouse striatal lysates following viral mediated eGFP or PIAS1 treatment. Insoluble PIAS1 levels are significantly increased following PIAS1 treatment in R6/2, but not NT mice compared to eGFP treatment. All data are expressed as western quantitation and relative expression to NT + eGFP treated mice. Protein expression was validated for protein loading prior to antibody incubation using reversible protein stain and each samples' corresponding soluble a-tubulin expression. Densitometry analyses for (C) and (D) revealed increased levels of PIAS1 compared to age- and sex-matched NT littermates. Data represent mean ± SEM. $^{*}p<0.05$; $^{**}p<0.01$; $^{***}p<0.001$, $^{****}p<0.0001$; One-way ANOVA followed by Bonferroni post-testing testing was applied. n=4/treatment. *See also* Figures S1, S3, and S5.

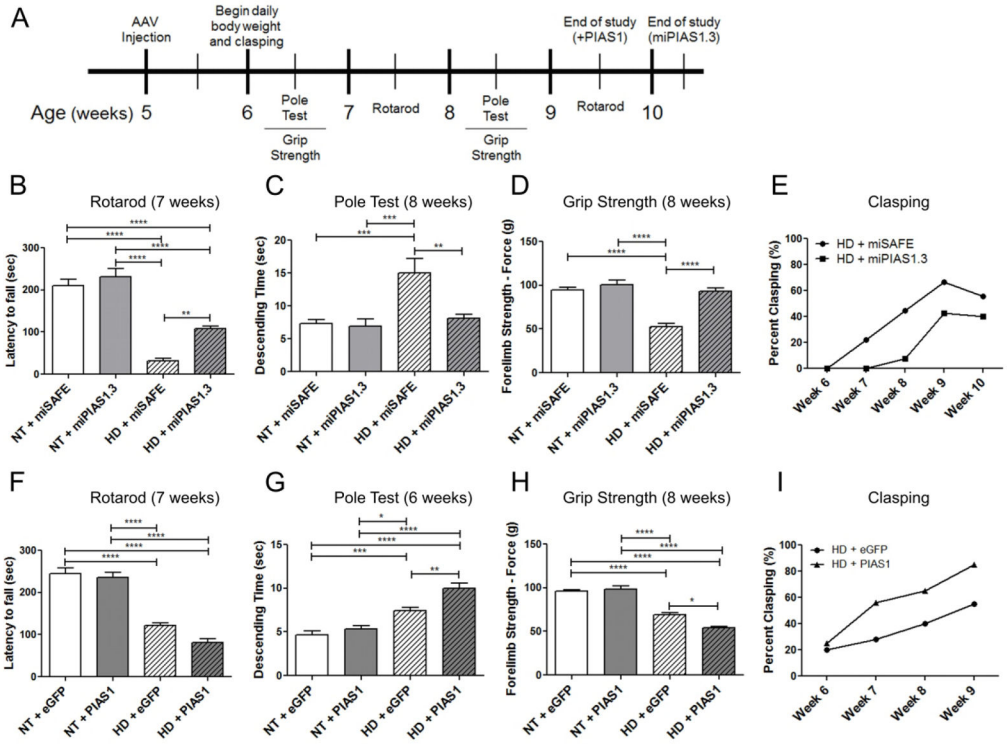

Figure 2. Effects of PIAS1 modulation on behavior in R6/2 mice

(A) Timeline of the study shows age of mice at treatment and timing of behavioral testing (n=10 per group) assessed through clasping, Rotarod, pole test, and grip strength. (B–E) PIAS knockdown: 7-week (Rotarod) and 8-week (pole test and grip strength) old mice are shown. R6/2 mice treated with miSAFE performed significantly worse on all tasks compared to NT + miSAFE/miPIAS1.3. R6/2 mice injected with miPIAS1.3 virus demonstrated improvements in clasping over time. Behavioral deficits were significantly improved in HD + miPIAS1.3 compared to HD + miSAFE on Rotarod time, descent time, and forelimb grip strength. (F–I) PIAS overexpression: 7-week (Rotarod), 6-week (pole test), and 8-week (grip strength) old mice are shown. R6/2 mice treated with eGFP performed significantly worse on all tasks compared to NT + eGFP/PIAS1. R6/2 mice injected with +PIAS1 virus demonstrated exacerbated deficits in clasping over time. Behavioral deficits were significantly worsened in R6/2 + PIAS1 compared to R6/2 + eGFP in descending time and forelimb grip strength. No significant treatment effect was detected for eGFP v. PIAS1 overexpression in R6/2 mice for Rotarod latency to fall time. *P<0.05, **P<0.01, ***P<0.001, ****P<0.0001 values represent means ± SEM. Statistical significance was determined by one-way ANOVA with Bonferroni post-testing for all behavioral analysis. *See also* Figures S4, S6,, S7, and S8.

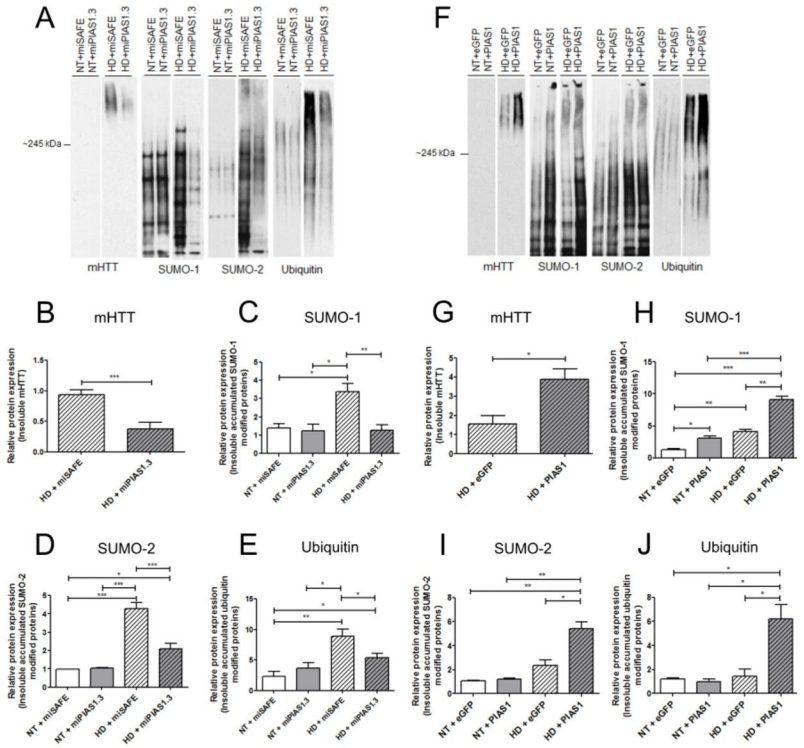

Figure 3. PIAS1 modulates insoluble protein accumulation in R6/2 mice

Western blot analysis of mouse striatal lysates separated into detergent-soluble and detergent-insoluble fractions. (A) PIAS knockdown: R6/2 mouse striatum is enriched in insoluble accumulated mHTT and SUMO-1, SUMO-2, and ubiquitin conjugated proteins compared to NT mice at 10 weeks. PIAS1 knockdown in R6/2 mice results in a significant reduction of insoluble (B) HMW accumulated HTT, (C) SUMO-1 and (D) SUMO-2 insoluble conjugated proteins, and a decrease in (E) ubiquitin-modified insoluble conjugated proteins compared to R6/2 miSAFE treated mice. Quantitation of the relative protein expression for mHTT, SUMO-1, SUMO-2 and Ubiquitin is shown directly below blots in A. (F) PIAS1 overexpression in R6/2 mice results in a significant increase of insoluble (G) HMW accumulated mHTT, (H) SUMO-1 and (I) SUMO-2 insoluble conjugated proteins, and an increase in (J) ubiquitin-modified insoluble conjugated proteins compared to eGFP treated R6/2 mice. Quantitation of the relative protein expression for mHTT, SUMO-1, SUMO-2 and Ubiquitin is shown directly below blots in F. **P*<0.05, ***P*<0.01, ****P*<0.001 values represent means ± SEM. Statistical significance for relative insoluble accumulated mHTT expression was determined with a two-tailed Student's *t* test. One-way ANOVA followed by Bonferroni post-testing testing was applied for SUMO-1, SUMO-2, and ubiquitin accumulated proteins groups. n=4/treatment. *See also* Figure S2.

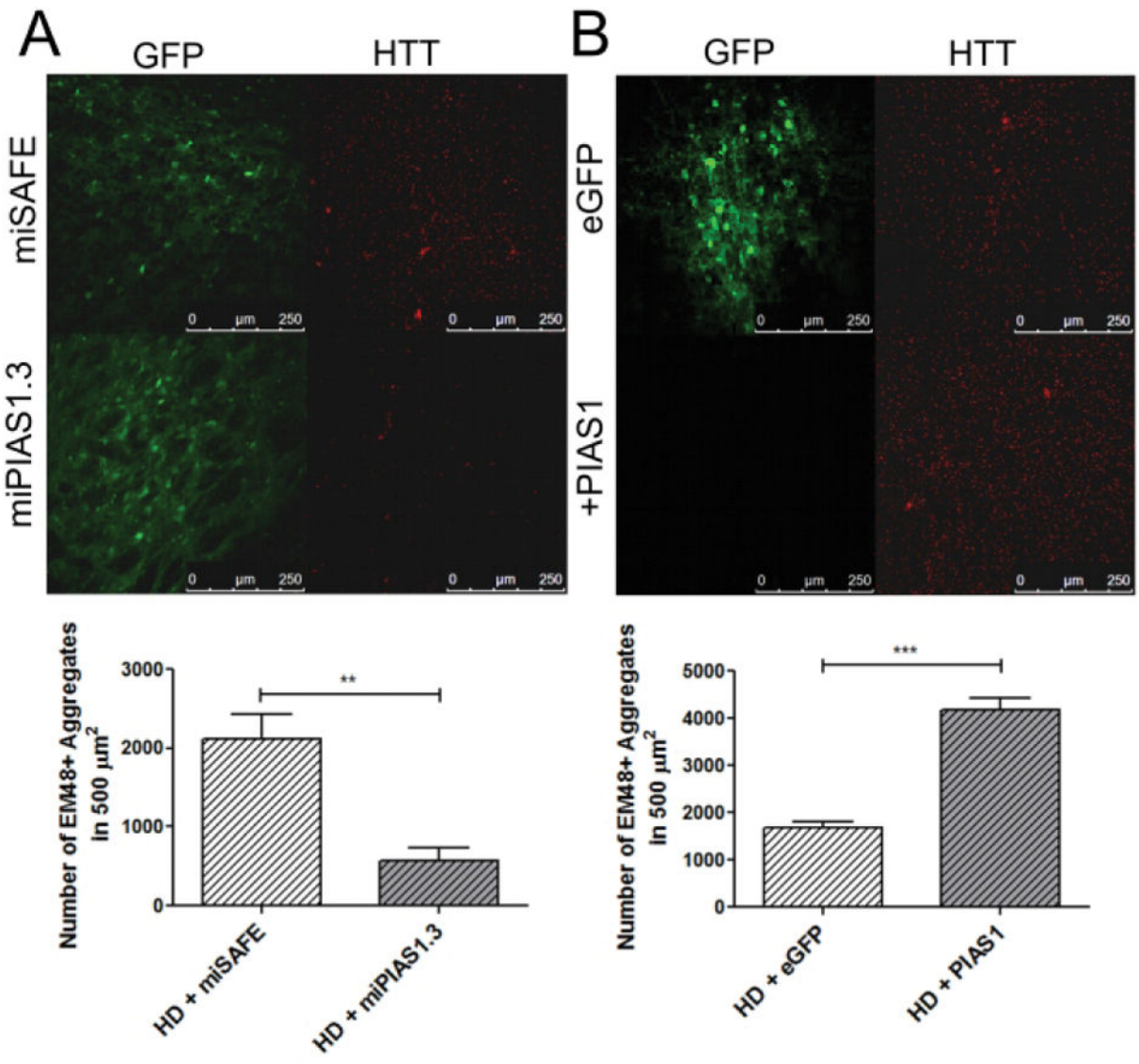

Figure 4. PIAS1 knockdown reduces mHTT inclusions in HD mouse striatum

Consecutive coronal brain sections containing striatum were immunostained against mHTT containing aggregates; anti-huntingtin (red) and viral reporter GFP expression (green). (A) Images (20x) show that animals with behavioral rescue associated with PIAS1 knockdown also showed a significant reduction in levels of EM48+ aggregates – red) in the striatum in comparison with miSAFE injected mice (n=3 mice) where virus was expressed (GFP - green) (quantitation shown below representative images). (B) R6/2 mice with PIAS1 overexpression showed a significant increase in levels of EM48+ aggregates – red) in the striatum in comparison with eGFP injected R6/2 mice (quantitation shown below representative images). ** P<0.01, *** P<0.001 values represent means ± SEM. Statistical significance for number of EM48+ aggregates was determined with a two-tailed Student's t test. Bars = 250 µm; n=4/treatment.

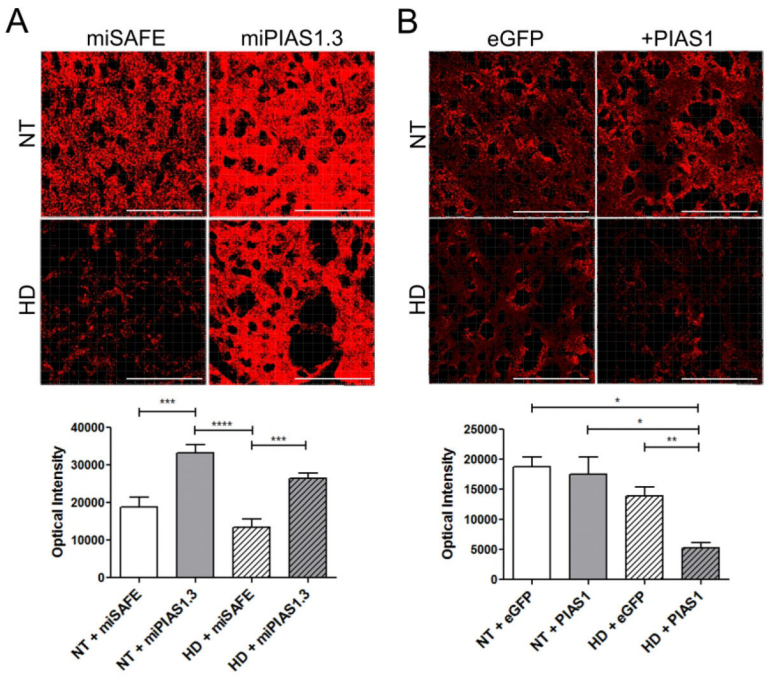

Figure 5. PIAS1 modulation alters levels of synaptophysin in the striatum of R6/2 mice

Confocal laser scanning microscopy images (63x) of immunofluorescence for synaptophysin in striatum of NT and R6/2 mice treated with miSAFE/miPIAS1.3 at 10 weeks of age (A) and NT and R6/2 mice treated with eGFP/PIAS1 at 9 weeks of age (B). Consecutive coronal brain sections containing striatum were stained against synaptophysin. Histograms describe the optical intensity levels of synaptophysin in neurons of the NT and R6/2 mice treated with miSAFE/miPIAS1.3 and NT and R6/2 mice treated with eGFP/PIAS1, respectively. There is a higher density of immunoreactivity in the NT mice relative to the R6/2 samples. Following treatment with miPIAS1.3, synaptophysin levels are significantly increased in both NT and R6/2 mouse striatum (representative images). PIAS1 overexpression significantly reduced synaptophysin levels in the striatum of R6/2 mice compared to eGFP treated mice (shown below representative images). *P<0.05, **P<0.01, ***P<0.001, ****P<0.0001 values represent means ± SEM. One-way ANOVA followed by Bonferroni post-testing testing was applied for all immunofluorescence analysis. Bars = 75 μm; n=4/treatment. *See also* Figure S9.

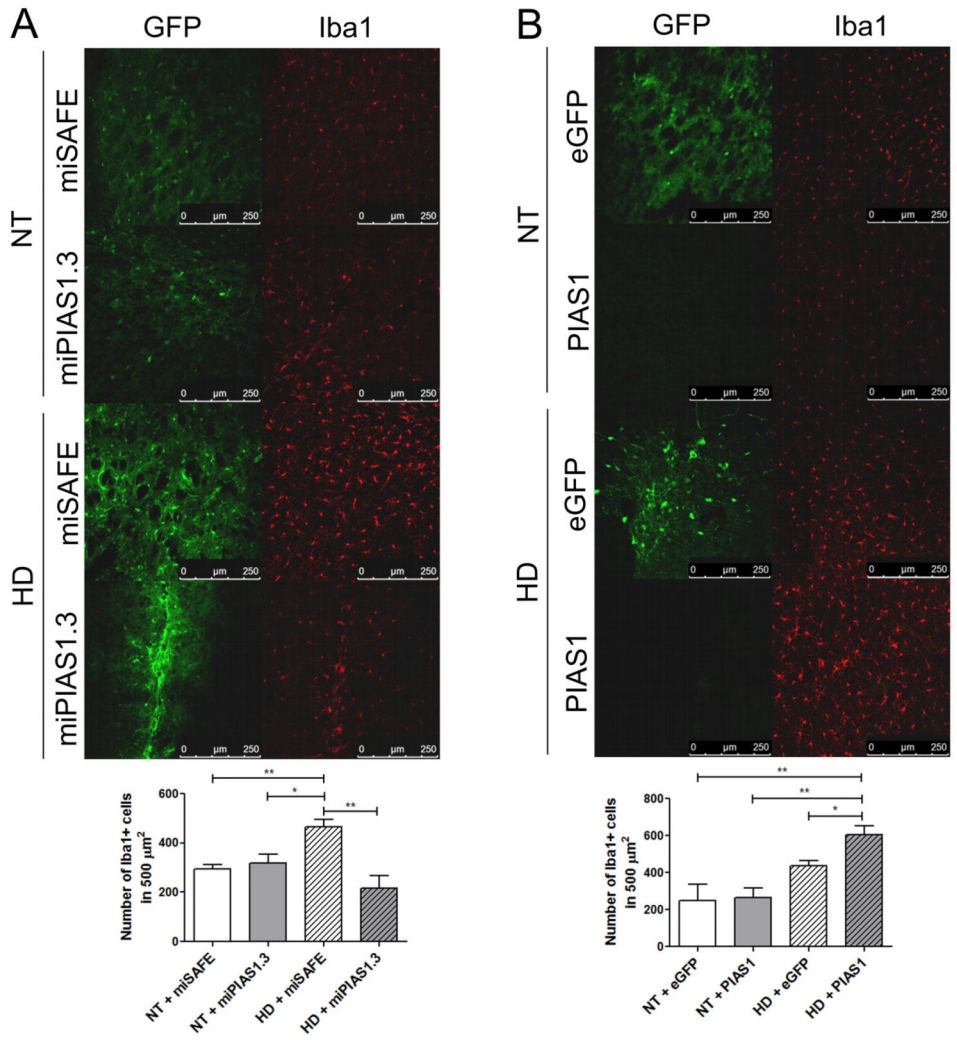

Figure 6. Iba1+ microglia numbers are decreased by PIAS1 reduction in the R6/2 striatum

Consecutive coronal brain sections containing striatum were stained against Iba1, a microglia marker. (A) Images (20x) show that R6/2 mice with behavioral rescue associated with PIAS1 knockdown also showed a significant reduction in levels of microglia (Iba1+ cells; red) in the striatum in comparison with miSAFE injected R6/2 mice (shown below representative images). (B) R6/2 mice with PIAS1 overexpression showed a significant increase in levels of microglia (Iba1+ cells; red) in the striatum in comparison with eGFP injected R6/2 mice (shown below representative images). **P*<0.05, ***P*<0.01, ****P*<0.001 values represent means ± SEM. Statistical comparisons of results were performed by performing one-way ANOVA analysis followed by Bonferroni's multiple comparison tests; Bars = 250 µm; n=4/treatment.

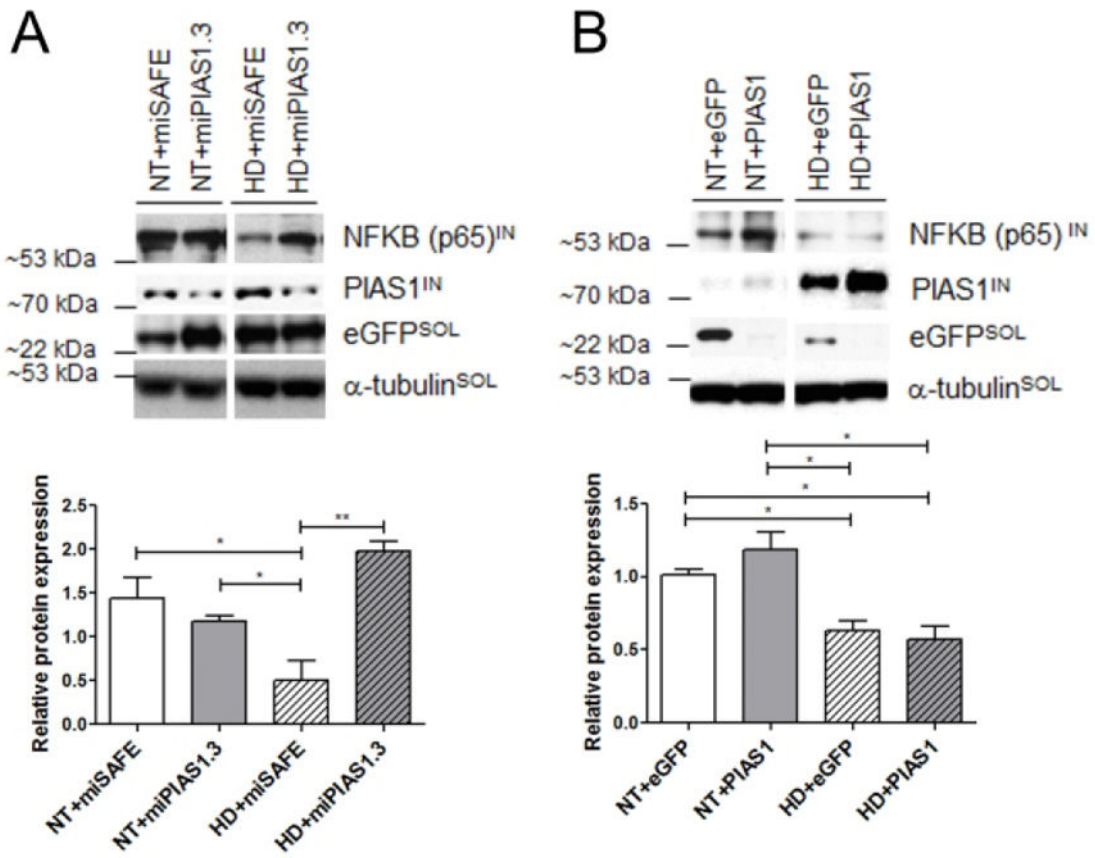

Figure 7. Insoluble NF-κB (p65) levels are restored to NT levels following PIAS1 reduction in the R6/2 striatum

(A–B) Western blot analysis of whole tissue mouse striatal lysates from R6/2 and NT mice. In both knockdown and overexpression studies, R6/2 mice exhibited significantly reduced levels of insoluble p65 compared to NT mice. (A) Striatal injections of miPIAS1.3 resulted in a significant knockdown of PIAS1 levels in both NT and R6/2 mice. PIAS1 knockdown in NT mice produced no significant alteration in levels of insoluble p65, whereas PIAS1 knockdown in R6/2 mice resulted in a significant increase. (B) PIAS1 overexpression in NT and R6/2 mice resulted in no significant alteration in levels of insoluble NF-κB p65. All data are expressed as western quantitation and relative expression to NT + miSAFE/eGFP treated mice. Protein expression was validated for protein loading prior to antibody incubation using reversible protein stain and each samples' corresponding soluble α-tubulin expression. $*P<0.05$, $**P<0.01$, values represent means ± SEM. Statistical comparisons of results were performed by performing one-way ANOVA analysis followed by Bonferroni's multiple comparison tests; n=4/treatment.

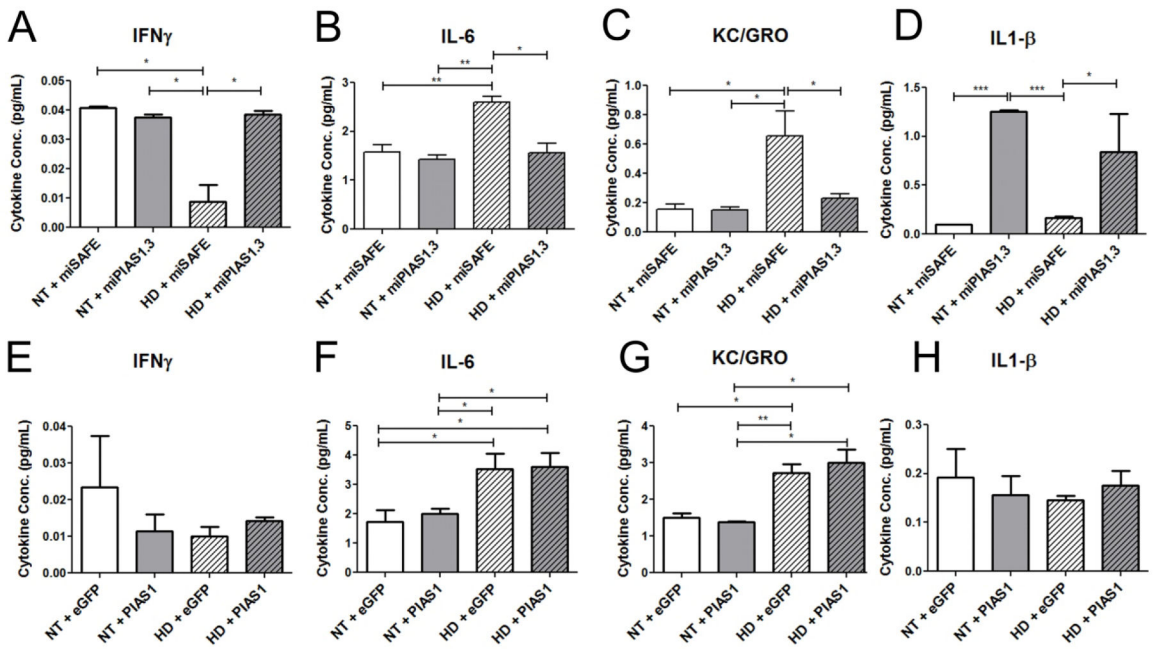

Figure 8. Soluble inflammatory cytokines are altered in the R6/2 striatum and restored to NT levels following PIAS1 knockdown

(A–H) Temporal profile of pro-inflammatory cytokines in detergent soluble fraction of striatal tissue homogenates. R6/2 mice contained significantly higher levels of IL-6 and KC/GRO, significantly reduced levels of IFNγ, and no change in IL1-β compared to NT mice. (A–D) PIAS1 knockdown resulted in significant changes in (A) IFNγ, (B) IL-6, and (C) KC/GRO concentrations (pg/ml) in R6/2 compared to miSAFE treated animals. PIAS1 knockdown significantly increased (D) IL1-β levels in both R6/2 and NT mice relative to miSAFE treated mice. (F) PIAS1 overexpression resulted in no significant alteration in (E) IFNγ (F) IL-6 (G) KC/GRO, and (H) IL1-β concentrations (pg/ml) in either R6/2 or NT mice compared to eGFP treated animals. *P<0.05, **P<0.01, ***P<0.001 values represent means ± SEM. Statistical comparisons of results were performed by performing one-way ANOVA analysis followed by Bonferroni's multiple comparison tests; n=4/treatment. *See also* Figure S10.